Available online at www.sciencedirect.com
SCIENCE DIRECT®
Thermochimica Acta 414 (2004) 35–42
thermochimica acta
www.elsevier.com/locate/tca

Tin(II)-EDTA complex: kinetic of thermal decomposition by non-isothermal procedures

Luciana S. Guinesi, Clóvis A. Ribeiro*, Marisa S. Crespi, Ana M. Veronezi

Departamento de Química Analítica, Instituto de Química, Universidade Estadual Paulista (UNESP), PO Box 355, Araraquara, 14801-970 Sao Paulo, Brazil

Received 16 December 2002; received in revised form 20 October 2003; accepted 20 October 2003

Abstract

Tin on the oxide form, alone or doped with others metals, has been extensively used as gas sensor, thus, this work reports on the preparation and kinetic parameters regarding the thermal decomposition of Sn(II)-ethylenediaminetetraacetate as precursor to SnO_2. Thus, the acquaintance with the kinetic model regarding the thermal decomposition of the tin complex may leave the door open to foresee, whether it is possible to get thin film of SnO_2 using Sn(II)-EDTA as precursor besides the influence of dopants added.

The Sn(II)-EDTA soluble complex was prepared in aqueous medium by adding of tin(II) chloride acid solution to equimolar amount of ammonium salt from EDTA under N_2 atmosphere and temperature of 50 °C arising the pH $\sim$ 4. The compound was crystallized in ethanol at low-temperature and filtered to eliminate the chloride ions, obtaining the heptacoordinated chelate with the composition $H_2SnH_2O(CH_2N(CH_2COO)_2)_2{\cdot}0.5H_2O$.

Results from TG, DTG and DSC curves under inert and oxidizing atmospheres indicate the presence of water coordinated to the metal and that the ethylenediamine fraction is thermally more stable than carboxylate groups. The final residue from thermal decomposition was the SnO_2 characterized by X-ray as a tetragonal rutile phase.

Applying the isoconversional Wall–Flynn–Ozawa method on the DSC curves, average activation energy: $E_a = 183.7 \pm 2.7$ and $218.9 \pm 2.1\,kJ\,mol^{-1}$, and pre-exponential factor: $\log A = 18.85 \pm 0.27$ and $19.10 \pm 0.27\,min^{-1}$, at 95% confidence level, could be obtained, regarding the loss of coordinated water and thermal decomposition of the carboxylate groups, respectively. The E_a and $\log A$ also could be obtained applying isoconventional Wall–Flynn method on the TG curves.

From E_a and $\log A$ values, Dollimore and Malék procedures could be applied suggesting R3 (contracting volume) and SB (two-parameter model) as the kinetic model to the loss of coordinated water (177–244 °C) and thermal decomposition of the carboxylate groups (283–315 °C), respectively. Simulated and experimental normalized DTG and DSC curves besides analysis of residuals check these kinetic models.

Keywords: Sn(II)-EDTA; Non-isothermal kinetics; Activation energy; Kinetic model

1. Introduction

1.1. Solid Sn-EDTA complex

Solids $Na_2Sn(II)Y{\cdot}2H_2O$, $Sn(II)_2Y{\cdot}2H_2O$ and $CaSn(II)Y{\cdot}4H_2O$, where Y = EDTA, were obtained by Langer [1] varying the metal:ligand ratio and it was observed, through infrared spectra, that the tin in these compounds can have 4 or 6 coordination number. The obtained sodium salt of a 1:1 chelate is a cyclic compound in which the metal is bonded to the nitrogen and acetates group. The 2:1 chelate is a linear complex in which it is possible the hydrogen bonding between water and carboxyl groups and still the inter or intra-molecular participation of both oxygen atoms of a carboxylate group in coordination to the metal.

Van Remoortere et al. [2] suggested, through X-ray diffraction, that the distannous complex $Sn(II)[Sn(II)Y{\cdot}H_2O]{\cdot}2H_2O$ crystallizes in the space group P1 with one formula weight in each triclinic unit cell. The geometry of the inner coordination sphere around tin is a distorted pentagonal bipyramid and the remaining sites are taken by oxygen from each of the four carboxylate substituents. Each SnY unit is bonded to four Sn(II) atoms of the second type via carboxylate oxygen's.

* Corresponding author. Fax: +55-162227932.
E-mail address: ribeiroc@iq.unesp.br (C.A. Ribeiro).

0040-6031/$ – see front matter © 2003 Elsevier B.V. All rights reserved.
doi:10.1016/j.tca.2003.10.011

The crystalline structure of stannic complex, Sn(IV)(OH_2)Y, was determined through X-ray diffraction [3]. It has been verified that the compound crystallizes in space group $P2_1/c$ with four formula units in each unit cell. Tin(IV) is coordinated by the two nitrogen atoms, four carboxylate oxygens of the hexadentate ligand and by the water molecule to form a seven-coordinate aqua complex.

1.2. Kinetic aspects

The mathematical description of the data from a single step solid state decomposition is usually defined in terms of a kinetic triplet, as activation energy, E_a, Arrhenius parameters, A, and an algebraic expression of the kinetic model in function of the fractional conversion α, $f(\alpha)$, which can be related to the experimental data as follows [4]:

$$\frac{d\alpha}{dt} = A \exp\left(-\frac{E}{RT}\right) f(\alpha) \quad (1)$$

For dynamic data obtained at a constant heating rate, $\beta = dT/dt$, this new term is inserted in Eq. (1) to obtain the transformation:

$$\frac{d\alpha}{dT} = \left(\frac{d\alpha}{dt}\right)\left(\frac{dt}{dT}\right) = \left(\frac{d\alpha}{dt}\right)\left(\frac{1}{\beta}\right) \quad (2)$$

$$\frac{d\alpha}{dT} = \frac{A}{\beta} \exp\left(-\frac{E}{RT}\right) f(\alpha) \quad (3)$$

The dynamic experiments can be more convenient to carry out if compared to running isothermal experiments and the reason for that is it takes time to reach an isothermal temperature [5]. However, any disagreement between data obtained from dynamic and isothermal experiments has been argued in literature [6].

The activation energy from dynamic data may be obtained from isoconversional method of Flynn and Wall [7] and Ozawa [8,9] using the Doyle's approximation of $p(x)$ [10], which involves measuring the temperatures corresponding to fixed values of α from experiments at different heating rates, plotting $\ln(\beta)$ against $1/T$:

$$\ln(\beta) = \ln\left[\frac{AE}{Rg(\alpha)}\right] - 5.331 - 1.052\frac{E}{RT} \quad (4)$$

This method allows to obtain the activation energy, $E = E(\alpha)$ independently of the kinetic model.

The pre-exponential factor is evaluated taking into account that the reaction is a first-order one and can be defined as [11]:

$$A = \frac{\beta E}{RT_m^2} \exp\left(\frac{E}{RT_m}\right) \quad (5)$$

1.2.1. Kinetic model determination

The rate of the kinetic process $d\alpha/dt$ through DSC curves is based on the relation:

$$\frac{d\alpha}{dt} = \frac{\phi}{\Delta H_c} \quad (6)$$

where ϕ is the heat flow normalized per sample mass and ΔH_c corresponds to the enthalpy change associated with this process.

The rate of the kinetic process can be expressed by:

$$\frac{d\alpha}{dt} = K(T) \cdot f(\alpha) \quad (7)$$

where

$$K(T) = A \exp\left(-\frac{E_a}{RT}\right) \quad (8)$$

The shape of a dynamic DSC curve at an specific heating rate considering any kind of model can be written as:

$$\phi = \Delta H_c A \exp\left(-\frac{E_a}{RT}\right) f(\alpha) \quad (9)$$

The test to find the kinetic model proposed by Malek [12–15] is based on this equation and on the normalized $y(\alpha)$ and $z(\alpha)$ functions, that, under non-isothermal conditions, they are given by:

$$y(\alpha) = \phi \exp\left(\frac{E_a}{RT}\right) = B_n f(\alpha) \quad (10)$$

where $B_n = \Delta H_c A$ is constant and the shape of the $y(\alpha)$ function is formally identical to the kinetic model $f(\alpha)$ in which the maximum value is α_y^* [12,15]

$$z(\alpha) = \phi T \pi\left(\frac{E_a}{RT}\right) = \Delta H_c \beta f(\alpha) g(\alpha) \quad (11)$$

where $\pi(E_a/RT)$ is an approximation of the integral temperature [16] that, in case of the $z(\alpha)$ function [17], can be obtained accurately considering the approximation $\pi \approx RT/E_a$, then:

$$z(\alpha) = \phi T^2 = C_n f(\alpha) g(\alpha) \quad (12)$$

where $C_n = \Delta H_c \beta E_a / R$ is constant and the α at the maximum of the $z(\alpha)$, α_z^*, is characteristic for any kinetic model [12,15].

The kinetic models to some thermal decomposition reactions can also be obtained through Dollimore's method, which is based on the "sharpness" of the onset (T_i) and final (T_f) temperatures of the TG/DTG and its asymmetry [18,19]. The investigation of some parameters that describe this asymmetry can thereby indicate the probable kinetic mechanism expressed as $f(\alpha)$. When the thermal decomposition reaction is not complex, the quantitative approach may be obtained using parameters such as α_{max} or $(d\alpha/dT)_{max}$, peak temperature (T_p), half-width from DTG curves.

This work aims at the kinetic evaluation of E_a and A to the coordinated water dehydration and thermal decomposition of the carboxylate groups to the Sn(II)-EDTA complex and their kinetic models through non-isothermal methods described above based on the TG, DTG and DSC curves.

2. Experimental

2.1. Chemicals

The metal, inorganic salts, acids and solvents used to prepare the complex were reagent grade. The EDTA, in acid form, and metallic tin were purchased from Analyticals-Carlo Erba Co. Ammonium carbonate and chloridric acid were purchased from Merck. Anhydrous ethanol was previously purified in our labor.

2.2. Preparation of the solid tin(II)-EDTA complex

The 2.646 mmol of tin(II) chloride acid solution was added to an equimolar amount of ammonium ethylenediaminetetraacetate solution under N_2 atmosphere (to avoid the hydrolysis of the metallic cation) and at a temperature of 50 °C. The soluble chelate was obtained after the addition of ammonium carbonate saturated solution up to pH ∼ 4. The crystalline solid Sn(II)-EDTA complex was obtained after a slow addition of an (10:1) ethanol:water solution at low-temperature. After total sedimentation, around 12 h, the white solid Sn(II)-EDTA complex was filtered and washed with ethanol until the elimination of the chloride ions, then dried at room temperature and stored in a desiccator containing anhydrous $CaCl_2$ (yields, 70%). The obtained compound was the $H_2SnH_2O(CH_2N(CH_2COO)_2)_2{\cdot}0.5H_2O$ (M chelate) = 435.94 g mol^{-1}. Calculated: C, 27.55%; H, 3.93%; N, 6.43%. Found: C, 27.64%; H, 4.29%; N, 6.56%.

2.3. Characterization

The complex was characterized through infrared absorption spectra (IR) in the 4000–200 cm^{-1} region by using a Spectrum 2000 spectrophotomer as CsI pellet and through elemental analysis (N, H, C) by using CE Instruments equipment, model EA 1110-CHNS-O. The residue oxide was characterized through DRX using a Siemens D 5000 diffractometer with Cu Kα radiation, submitted to 40 kV, 30 mA, 0.05° s^{-1} step and exposed to radiation from 4° up to 70° (2θ). The TG/DTG–DTA experiments were performed using a simultaneous module of thermal analysis, SDT 2960 from TA Instruments, under dynamic atmosphere of nitrogen and synthetic air (100 ml min^{-1}), alumina crucible of 40 μl, α-Al_2O_3 as reference material, sample mass around 6 mg and heating rates of 5, 10 and 20 °C min^{-1} from 40 up to 1200 °C. DSC recording was obtained by using a DSC 2910 module from TA Instruments under dynamic atmosphere of nitrogen (100 ml min^{-1}), covered aluminum crucible of 10 μl with sample mass around 2 mg, aluminum crucible as reference material and heating rates of 5, 10 and 20 °C min^{-1} from 40 up to 600 °C. The E_a and log A kinetic parameters were calculated through the software's TGAKin V4.04 and DSCASTMKin V4.08 from TA Instruments.

3. Results and discussion

Data from IR spectra to the compound showed three broadening bands with medium intensity at 3535, 3438 and 3257 cm^{-1} due to the C–H and O–H stretching in the CH_2 groups of the EDTA and water molecules, respectively [20–22]. A very strong band at 1680 cm^{-1} and a medium ones at 931 cm^{-1} are due to C=O asymmetric and acetate C–C stretching, respectively [20–24]. The appearance of these two bands as a single sharp line is an evidence for the equivalence of the carboxylate groups, which would be four coordinated to the metal [20,22,23]. Medium and weak bands at 1444 and 1130 cm^{-1} have been assigned to C=O symmetric and C–N stretching, respectively [20–22].

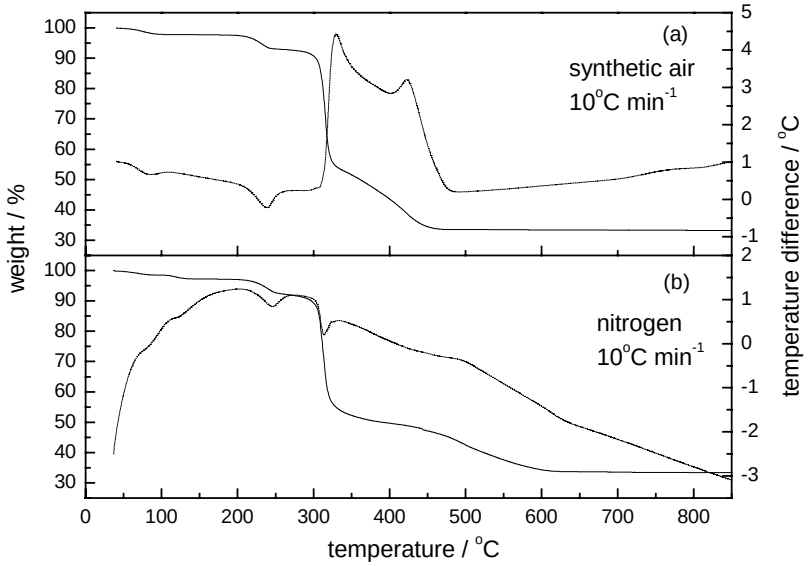

Fig. 1. TG–DTA curves to $H_2SnH_2O(CH_2N(CH_2COO)_2)_2{\cdot}0.5H_2O$ compound in (a) synthetic air and (b) nitrogen atmosphere.

A weak additional band at 410 and 350 cm^{-1} are associated with νSn–O and νSn–N vibrations, respectively [21,24]. From IR spectrum data, TG curves and elemental analysis it could be suggested that the metal is coordinated to nitrogen atoms, to four carboxylate groups of the EDTA and to a water molecule as a heptacoordinated compound, $H_2SnH_2O(CH_2N(CH_2COO)_2)_2{\cdot}0.5H_2O$.

Fig. 1 depicts the TG and DTA curves of the complex obtained under synthetic air and nitrogen atmospheres and at 10 °C min^{-1}. In both atmospheres, the observed mass loss between 40 and 105 °C, with a corresponding endothermic peak at 84.8 °C, may be ascribed to the loss of 0.5 molecule of hydration water. The second thermal event between 200 and 245 °C (synthetic air atmosphere) and 205 and 254 °C (nitrogen atmosphere), may be related to the loss of $1H_2O$ coordinated to the metal with corresponding endothermic peaks at 239 and 246 °C, respectively. The oxidizing atmosphere provides the decomposition/oxidation of the ligand in two steps between 283 and 469 °C with two intense exothermic peaks at 327 and 423 °C with formation of the SnO_2 in the rutile phase over 480 °C as revealed by the X-ray diffraction patterns data. In the inert atmosphere, mass loss between 279 and 327 °C (36.52%), with a corresponding endothermic peak at 313 °C, can be observed. It may be due to the partial thermal decomposition of carboxylate groups owing to they present weaker bonds regarding the ethylenediamine group. The remainder complex, $Sn(CH_2N)_2CH_2COO$, show slow decomposition (18.51%) up to 625 °C likewise with formation of SnO_2.

Thus, the final residue is SnO_2, in the rutile phase, in both air and nitrogen atmosphere, nevertheless with a likely dissimilar mechanism, as indicated by the feature of the TG and DSC curves.

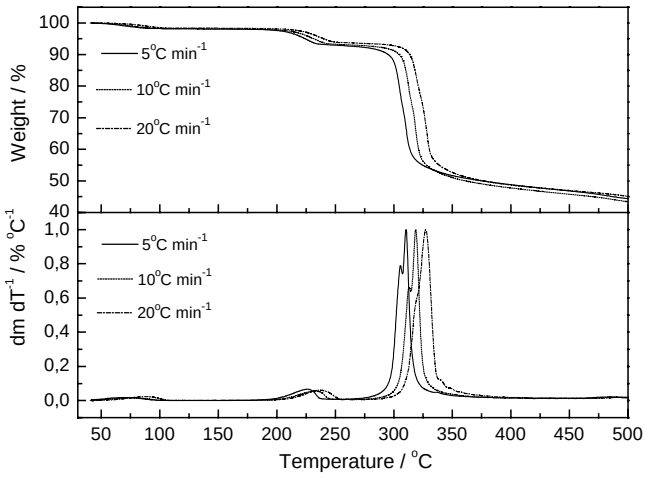

Fig. 2. TG and DTG curves to the $H_2SnH_2O(CH_2N(CH_2COO)_2)_2{\cdot}0.5H_2O$ compound in nitrogen atmosphere.

3.1. Calculation of the activation energy and pre-exponential factor

In the TG–DTG curves (Fig. 2) in nitrogen atmosphere, it can be seen the mass loss regarding coordinated water (187–250 °C) and thermal decomposition of the carboxylate groups (271–336 °C). The DSC curves (Fig. 3) show endothermic peaks with similarities to the TG–DTG curves (Fig. 2).

The kinetic parameters E_a and $\log A$ to the dehydration and first thermal decomposition were obtained applying the isoconversional method of Flynn and Wall [7] and Ozawa [8,9] on the reaction limits defined by TG and DSC curves. To each fixed fractional conversion, α, and correspondent temperature, the E_a could be calculated from the slope of plot

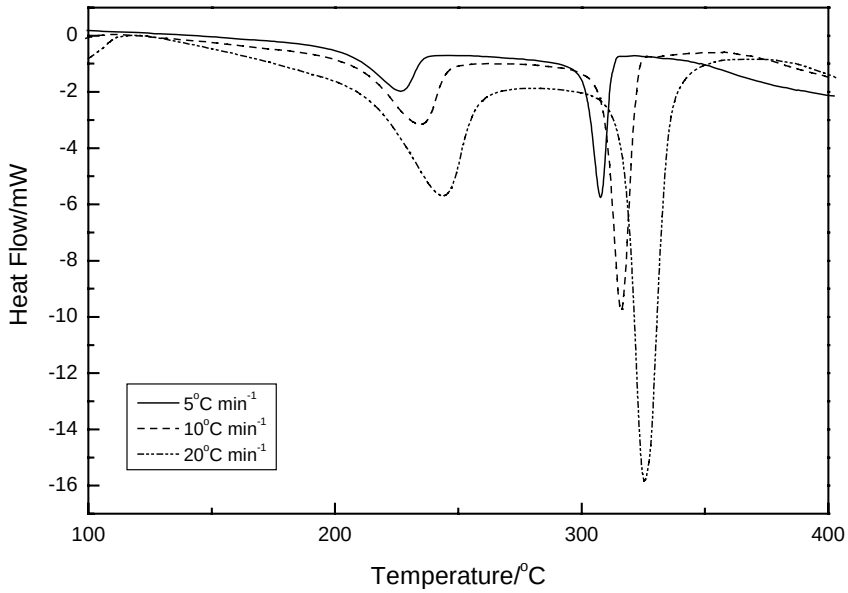

Fig. 3. DSC curves to the $H_2SnH_2O(CH_2N(CH_2COO)_2)_2{\cdot}0.5H_2O$ compound in nitrogen atmosphere.

Table 1
Data from TG and DSC used to obtain the thermal decomposition kinetic parameters E_a and $\log A$ regarding coordinated water (186–261 °C) and carboxyl group (265–344 °C) of the Sn(II)-EDTA complex

TGA curves (reaction limits)				DSC curves (reaction limits)			
β (°C min^{-1})	Start (°C)	Stop (°C)	Weight loss (%)	β (°C min^{-1})	Start (°C)	Stop (°C)	ΔH (J g^{-1})
4.98[a]	186.5	236.8	4.6	5.00[a]	203.6	235.6	−152.4
4.98[b]	271.2	317.0	34.9	5.03[b]	265.5	316.7	−217.3
9.99[a]	196.2	244.4	4.3	10.00[a]	213.3	245.3	−98.6
9.95[b]	278.5	327.1	36.5	9.99[b]	281.7	326.5	−253.8
19.50[a]	203.5	250.0	4.0	20.09[a]	218.1	261.5	−106.1
19.83[b]	287.2	336.1	36.6	19.77[b]	297.9	344.3	−257.3

[a] Loss of the coordinated water.
[b] Thermal decomposition of the carboxylate group.

of $\ln(\beta)$ against $1000/T$ (Eq. (4)) and then the corresponding $\log A$ through Eq. (5). The obtained results must be within the limit to be used the Doyle approximation to $p(x)$ in which the $20 \leq E/RT \leq 50$. Thus, the average values, at 95% confidence level, found to E_a and $\log A$ regarding the loss of coordinated water were 174.6±4.5 and 183.7±2.7 kJ mol^{-1}, and 17.64±0.57 and 18.85±0.27 min^{-1}, from TG and DSC curves, respectively. Regarding the thermal decomposition of the carboxylate groups of the complex, the average values obtained to E_a and $\log A$, through TG and DSC curves, were 200.5 ± 11.7 and 218.9 ± 2.1 kJ mol^{-1}, and 16.75 ± 1.2 and 19.10 ± 0.27 min^{-1}, respectively.

3.2. Determination of the kinetic model

3.2.1. Dollimore's procedure

Dollimore's procedure is applied on the curves TG/DTG whose asymmetry observed between the onset T_i and the final T_f in DTG curves, may be associated with the parameters as the fraction at rate of maximum decomposition, α_{max}, peak temperature, T_p, at $(d\alpha/dT)_{max}$, and HW = HiT–LoT which is the difference between the high-temperature and low-temperature at half-width of the DTG peak (Table 1).

Table 2
Data from DTG curves regarding the mass loss of the coordinated water

β (°C min^{-1})	T_p (°C)	α_{max}	Half-width peak, HW
4.98	226.0	0.67	22.62
9.99	231.9	0.63	24.56
19.50	236.0	0.58	25.51
Expected values to R3 model[a]		≥0.6 to <0.7	20–42

[a] T_i: diffuse, T_f: sharp.

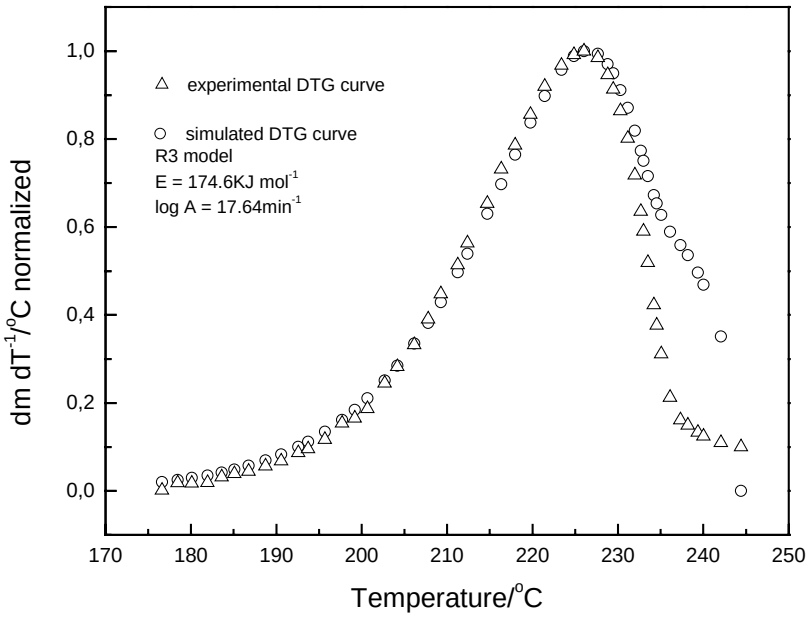

Fig. 4. Experimental and simulated DTG curves at 5 °C min^{-1} regarding the loss of coordinated water.

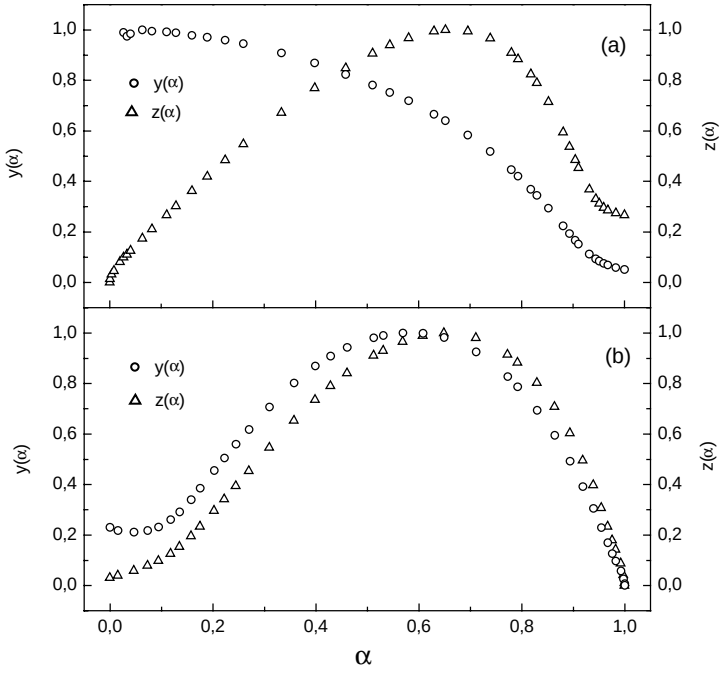

Fig. 5. The $y(\alpha)$ and $z(\alpha)$ functions calculated from DSC data (Fig. 3) regarding the (a) loss of coordinated water and (b) thermal decomposition of the carboxylate group.

To the loss of the coordinated water (Fig. 2) the investigation of these parameters [18,19] yields α_{max} at T_p and HW. Table 2 indicates the R3 model ($f(\alpha) = (1-\alpha)^{2/3}$), corresponding to the contracting volume reaction. Knowing the averages E_a and $\log A$, $\alpha - T$ relation and $f(\alpha)$, the corresponding normalized simulated $d\alpha/dT$ versus T plot could be obtained and compared with the normalized experimental DTG curve confirming that the loss of coordinated water follows the contracting volume, R3 model (Fig. 4).

Applying the Malek's procedure [12–15] to the data from DSC curves (Fig. 3) the kinetic model regarding the loss of the coordinated water and the first thermal decomposition reactions could be defined through the $y(\alpha)$ and $z(\alpha)$ functions, as defined in Eqs. (10) and (12), against α (Fig. 5a). The reaction, considering the mass loss of coordinated water, presents a maximum of the $z(\alpha)$ function, α_z^*, located at 0.65 and the $y(\alpha)$ function present its maximum, α_y^*, located at zero and a convex feature [$y(\alpha_I) > \alpha_I$] (Fig. 5a). This

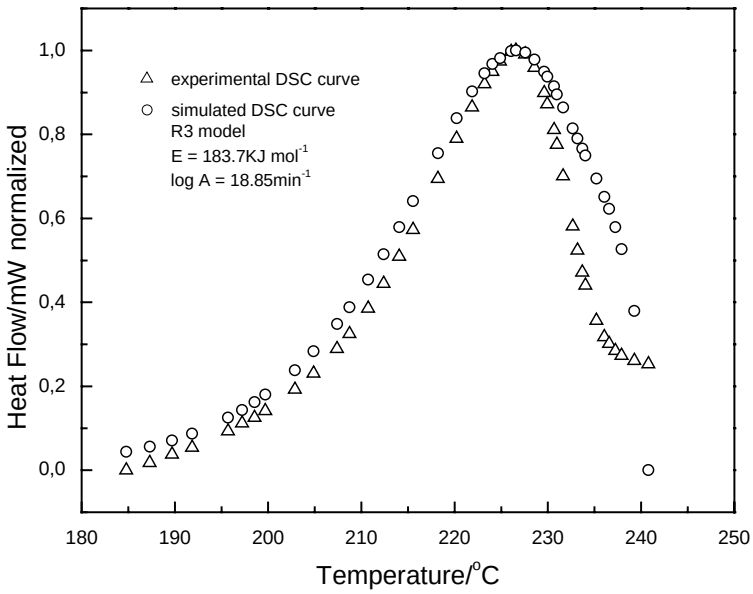

Fig. 6. Experimental and simulated DSC curves at 5 °C min^{-1} regarding the loss of coordinated water.

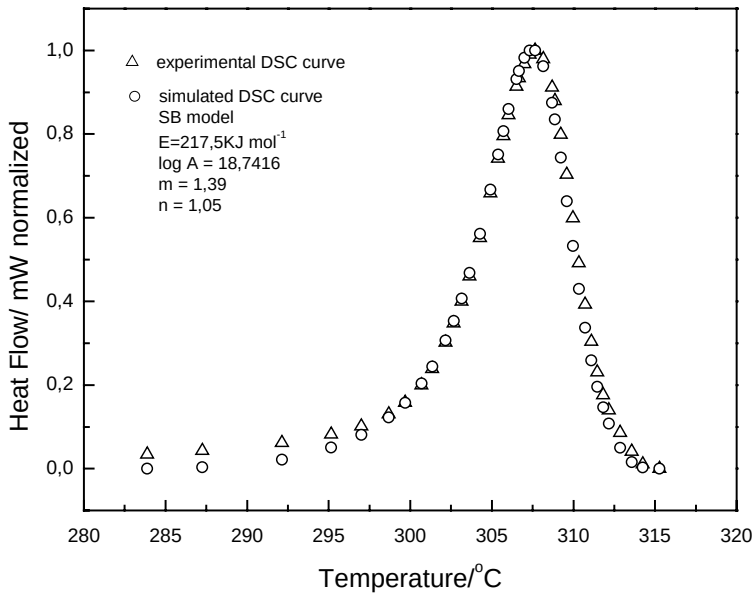

Fig. 7. Experimental and simulated DSC curves at $5\,^{\circ}\mathrm{C\,min^{-1}}$ regarding the thermal decomposition of the carboxylate groups.

behavior is characteristic to the R3 model [RO($n < 1$) model] and according to that found by Dollimore's procedure. As to the thermal decomposition of the carboxyl group at a heating rate of $5\,^{\circ}\mathrm{C\,min^{-1}}$, the $\alpha_y^* \approx 0.57$ and $\alpha_z^* \approx 0.65$ (Fig. 5b). In spite of appearing the α_z^* round 0.63, which is close to the value that would be expected for the JMA model, it has to be taken in account that the compound cannot be consider properly homogeneous. Thus, knowing that $0 < \alpha_y^* < \alpha_z^*$, the auto catalytic SB (Sesták–Berggren) model in which $f(\alpha) = \alpha^m(1-\alpha)^n$ seems to be the most suitable.

The kinetic exponent n of the SB model can be obtained by the slope of the linear regression from plot of $\ln[(\mathrm{d}\alpha/\mathrm{d}t)\exp(E/RT)]$ against $\ln[\alpha^p(1-\alpha)]$ for α values between 0.2 and 0.8 that yields $n = 1.05$. The kinetic exponent m then can be calculated by the relation $m = pn$, where $p = \alpha_y^*/(1-\alpha_y^*)$. Thus, the found value to m was 1.39.

The normalized simulated ϕ against T plot obtained through Eq. (9) and its proximity with the experimental DSC curves confirms the R3 (Fig. 6) and SB (Fig. 7) as the kinetic models to the loss of the coordinated water and thermal decomposition of the carboxylate groups, respectively. Residuals analysis (Figs. 8 and 9) allow to verify that there are not significant lack of fit of the simulated to experimental DSC and DTG curves, respectively.

As to the loss of the coordinated water, it can be observed a deviation from simulated to experimental DTG and DSC curves (Figs. 4 and 6) from $\alpha \approx 0.8$ and it may be due to an alteration in activation energy at the end of the process and/or

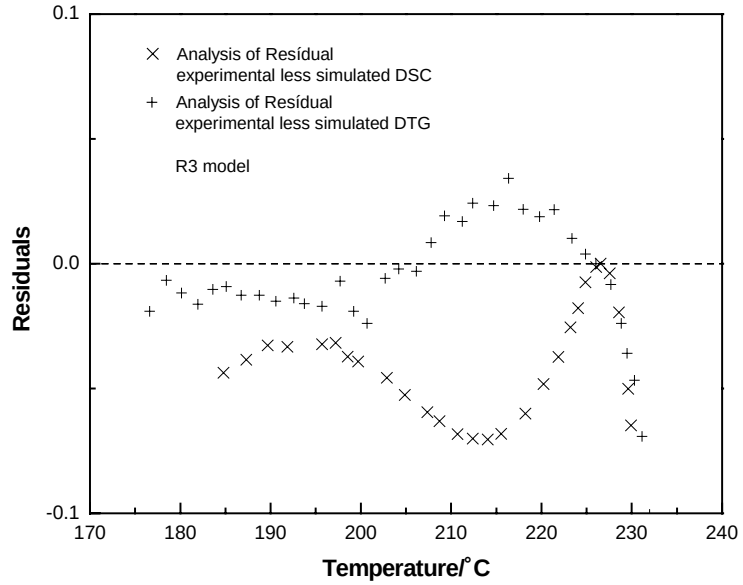

Fig. 8. Analysis of residual between experimental and simulated DSC and DTG curves regarding the loss of coordinated water.

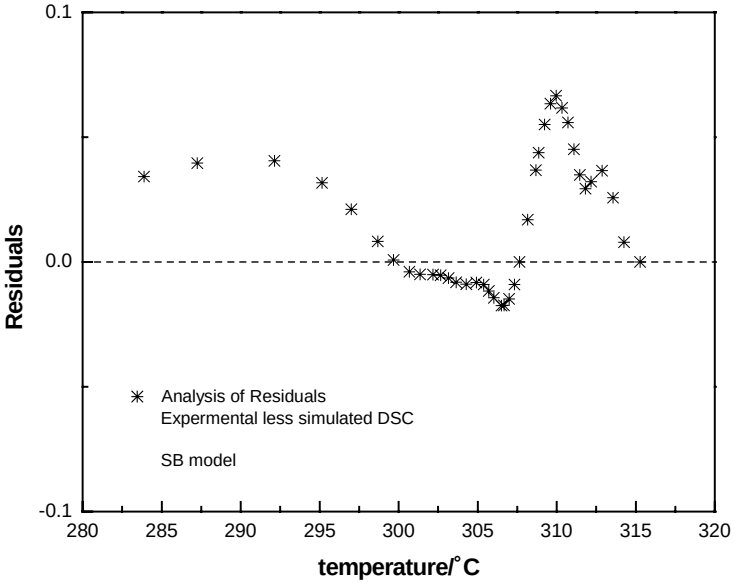

Fig. 9. Analysis of residual between experimental and simulated DSC curves regarding the thermal decomposition of the carboxylate groups.

influence of the succeeding thermal decomposition reaction. However, that deviation to the thermal decomposition of the carboxylate groups, despite the more complex reaction, could not be observed.

4. Conclusion

Besides the strong kinetic dependence on the experimental condition in a dynamic procedure, it can be seen from the resemblance between simulated and experimental normalized DTG and mainly DSC curves, that the kinetics parameters could be obtained even though they were originated from a thermal decomposition reaction, where there might have been the feedback of the gas phase produced under the reaction itself.

The kinetic model used in the Dollimore's procedure just consider the formal mathematical description of an ideal process, thus, in the case of the thermal decomposition of the carboxylate groups could not be successfully described by some set of ideal models. Malek's procedure make use of the same kinetics model than Dollimore's; nevertheless, the n and m are now defined as kinetic exponents and may not be the reaction's order.

Residuals analysis suggested that the mechanistic R3 and SB models show the best fit to the loss of coordinated water and thermal decomposition of carboxylate groups, respectively.

Acknowledgements

The authors acknowledge the CAPES by the financial support.

References

[1] H.G. Langer, J. Inorg. Nucl. Chem. 26 (1964) 767.
[2] F.P. Van Remoortere, J.J. Flynn, F.P. Boer, P.P. North, Inorg. Chem. 10 (1971) 1511.
[3] F.P. Van Remoortere, J.J. Flynn, F.B. Boer, Inorg. Chem. 10 (1971) 2313.
[4] M.E. Brown, D. Dollimore, A.K. Galwey, Reaction in the Solid State: Comprehensive Chemical Kinetics, vol. 22, Elsevier, Amsterdam, 1980.
[5] D. Dollimore, P. Phang, Anal. Chem. 72 (2000) 27R–36R.
[6] S. Vyazovkin, C.A. Wight, Thermochim. Acta 340–341 (1999) 53–68.
[7] J.H. Flynn, J. Wall, Nat. Bur. Stand. 70A (1966) 487.
[8] T. Ozawa, Bull. Chem. Soc. Jpn. 38 (1965) 1881.
[9] T. Ozawa, J. Therm. Anal. 2 (1970) 301.
[10] C. Doyle, J. Appl. Polym. Sci. 6 (1962) 639.
[11] H.E. Kissinger, Anal. Chem. 29 (1957) 1702.
[12] J. Malek, J. Sestak, F. Rouquerol, J. Rouquerol, J.M. Criado, A. Ortega, J. Therm. Anal. 38 (1992) 71.
[13] J. Malek, J. Therm. Anal. Cal. 56 (1999) 763.
[14] J. Malek, Thermochim. Acta 355 (2000) 239.
[15] J. Malek, J. Mater. Res. 16 (6) (2001) 1862.
[16] Sestak, Thermophysical Properties of Solids: Their Measurements and Theoretical Analysis, Elsevier, Amsterdam, 1984.
[17] J. Malék, Thermochim. Acta 267 (1995) 61.
[18] D. Dollimore, T.A. Evans, Y.F. Lee, F.W. Wilburn, Thermochim. Acta 188 (1991) 77–85.
[19] D. Dollimore, T.A. Evans, Y.F. Lee, G.P. Pee, F.W. Wilburn, Thermochim. Acta 196 (1992) 255.
[20] D.T. Sawyer, P.J. Paulsen, J. Am. Chem. Soc. 81 (1959) 816.
[21] A.A. McConnel, R.H. Nuttal, D.M. Stalker, Talanta 25 (1978) 425.
[22] M.F.G. Esteban, R.V. Serrano, F.G. Vilchez, Spectrochim. Acta 43A (1987) 1039.
[23] K. Krishnan, R.A. Plane, J. Am. Chem. Soc. 90 (1968) 3195.
[24] A.A. McConnel, R.H. Nuttal, Spectrochim. Acta 33A (1977) 459.